



Heterogeneous & Homogeneous & Bio- & Nano-

# CHEM **CAT** CHEM

---

## CATALYSIS

### Accepted Article

**Title:** Carbon with Surface-Enriched Nitrogen and Sulfur Supported Au Catalysts for Acetylene Hydrochlorination

**Authors:** Bolin Wang, Jia Zhao, Yuxue Yue, Gangfeng Sheng, Huixia Lai, Jiayao Rui, Haihua He, Zhongting Hu, Feng Feng, Qunfeng Zhang, Lingling Guo, and Xiaonian Li

This manuscript has been accepted after peer review and appears as an Accepted Article online prior to editing, proofing, and formal publication of the final Version of Record (VoR). This work is currently citable by using the Digital Object Identifier (DOI) given below. The VoR will be published online in Early View as soon as possible and may be different to this Accepted Article as a result of editing. Readers should obtain the VoR from the journal website shown below when it is published to ensure accuracy of information. The authors are responsible for the content of this Accepted Article.

**To be cited as:** *ChemCatChem* 10.1002/cctc.201801555

**Link to VoR:** <http://dx.doi.org/10.1002/cctc.201801555>

WILEY-VCH

[www.chemcatchem.org](http://www.chemcatchem.org)



# Carbon with Surface-Enriched Nitrogen and Sulfur Supported Au Catalysts for Acetylene Hydrochlorination

Bolin Wang<sup>[a]</sup>, Jia Zhao<sup>\*[a]</sup>, Yuxue Yue<sup>[a]</sup>, Gangfeng Sheng<sup>[a]</sup>, Huixia Lai<sup>[a]</sup>, Jiayao Rui<sup>[a]</sup>, Haihua He<sup>[a]</sup>, Zhongting Hu<sup>[b]</sup>, Feng Feng<sup>[a]</sup>, Qunfeng Zhang<sup>[a]</sup>, Lingling Guo<sup>[a]</sup>, Xiaonian Li<sup>\*[a]</sup>

**Abstract:** Nitrogen-doped carbons supported gold catalysts has attracted much attention in a broad range of applications. However, co-existence of multiple nitrogen species which may have vastly different effect on the gold-based catalysts, has limited the development of an ideal nitrogen-doped carbon support. Herein, we have demonstrated that by addition of sulfur species, selective formation of pyrrolic nitrogen against pyridinic nitrogen can be achieved for pyrrolic N-doped carbon support. The gold catalysts synthesized from the pyrrolic nitrogen doped carbon support produced using ionic liquid-assisted synthetic strategy (Au/N, S-AC-700), exhibited excellent catalytic activity and stability for hydrochlorination of acetylene. The outstanding performance was attributed to the  $\pi$  electrons transferred from pyrrolic nitrogen to Au (III) center, which could increase the electron density of Au hence facilitate the adsorption of hydrogen chloride on the catalyst.

## Introduction

Vinyl chloride is a monomer (VCM) for an important industrial material, polyvinyl chloride (PVC).<sup>[1,2]</sup> Hydrochlorination of acetylene catalyzed by carbon supported mercuric chloride (HgCl<sub>2</sub>/C) catalysts with typically mercury content of 10-15 wt%, is one of the most methods to manufacture VCM on an industrial scale. However, mercuric chloride is never a green catalyst due to its toxicity and volatility, inevitable mercuric chloride lost during the reaction can pose serious threat to the environment and human health.<sup>[2,3]</sup> Therefore, nonmercuric catalytic systems are urgently required in consideration of safety and green chemistry. To resolve this problem, a series of metal chlorides catalytic systems employing AuCl<sub>3</sub>,<sup>[4-6]</sup> PdCl<sub>2</sub>,<sup>[7,8]</sup> RuCl<sub>3</sub>,<sup>[9-12]</sup> and CuCl<sub>2</sub><sup>[13-15]</sup> as catalysts have been investigated by Hutchings *et al.* and many other research groups for acetylene hydrochlorination. Among the catalysts above, Au-based catalysts supported on activated carbon (AC) display the highest catalytic activity.<sup>[16]</sup> However, Au-based catalysts suffer unexceptionally from rapid catalyst deactivation because of the reduction of Au (III) complexes to Au<sup>0</sup> metal by acetylene, which confines its practical application.<sup>[17,18]</sup> Extensive efforts have been made to overcome this problem

and many of them have been focused on bimetallic Au-M catalysts (M= Pt,<sup>[7]</sup> Pd,<sup>[7]</sup> Ir,<sup>[7]</sup> Rh,<sup>[7]</sup> Co<sup>[19]</sup> and Bi<sup>[20]</sup>).

Meanwhile, some other literature reports have demonstrated that N-doped carbon supports are able to stabilize catalytic active Au(III) complexes by electrons transferred from dopant atoms to the Au(III) center, which facilitate the adsorption of hydrogen chloride to the catalyst.<sup>[21]</sup> However, effect of nitrogen dopants on the catalytic performance is highly dependent on the types of the dopants.<sup>[21-26]</sup> Pyrrolic nitrogen was believed to be an effective dopant which has conducive stabilization effect on cationic gold species.<sup>[21, 24-26]</sup> Bao *et al.* denoted that pyrrolic N is the only form of nitrogen dopant that has significant influence on the hydrochlorination reaction,<sup>[27]</sup> but co-existence of pyrrolic N and pyridinic N on the edge or defect of carbon surface is very common in nitrogen doped carbon materials.<sup>[28-31]</sup> What's worse, pyrrolic N species are unstable under high temperature, they could be transformed into more stable pyridinic N species if high-temperature treatment was used.<sup>[28,31-33]</sup> To the best of our knowledge, no solution has ever been reported for this problem. In addition, many of heteroatoms-containing precursors decompose into unstable substances under programmed heating conditions, resulting in a very low doping efficiency.<sup>[28]</sup> However, this nitrogen doping method is mostly used for bulk carbon doping which can not effectively catalyze the reaction.<sup>[24-26,34]</sup> Au sites involved in Au/C interfaces were considered to be the active sites for acetylene hydrochlorination,<sup>[35,36]</sup> which inspired us to consider replacing bulk doping with surface doping to improve the efficiency of the catalytic reaction in terms of "atom economy" and "green chemistry".

In this work, ionic liquids (ILs) were employed as heteroatom donors and a series of heteroatom-coated carbon supports were prepared. CH- $\pi$  bonds formed between the carbon atoms with high free  $\pi$ -electron density and the H atoms at the C2 position of cation in ILs was the linkers between the two substrates.<sup>[37]</sup> The 1-ethyl-3-methylimidazolium thiocyanate, [Emim][SCN], was firstly impregnated on the carbon surface and then the obtained IL/carbon was calcined at high temperature to form a carbon surface doped with enriched nitrogen and sulfur atoms. Subsequently, a series of gold-based catalysts were prepared by impregnation, and were characterized by SEM, TEM, BET, XRD, XPS, TPD and H<sub>2</sub>-TPR techniques to uncover the structural and electronic properties of the active sites. Interaction mechanism of nitrogen and sulfur species with carbon surface and their effects on the gold-based catalysts for acetylene hydrochlorination reaction was also studied.

[a] B. Wang, Prof. Dr. J. Zhao, Y. Yue, G. Sheng, H. Lai, J. Rui, H. He, F. Feng, Q. Zhang, L. Guo, Prof. Dr. X. Li  
Industrial Catalysis Institute, Laboratory Breeding Base of Green Chemistry-Synthesis Technology, Zhejiang University of Technology Hangzhou 310014, China  
E-mail: jiazhao@zjut.edu.cn, xnli@zjut.edu.cn

[b] Z. Hu  
College of Environment, Zhejiang University of Technology, Hangzhou 310014, China

Supporting information for this article is given via a link at the end of the document. ((Please delete this text if not appropriate))

## Results and Discussion

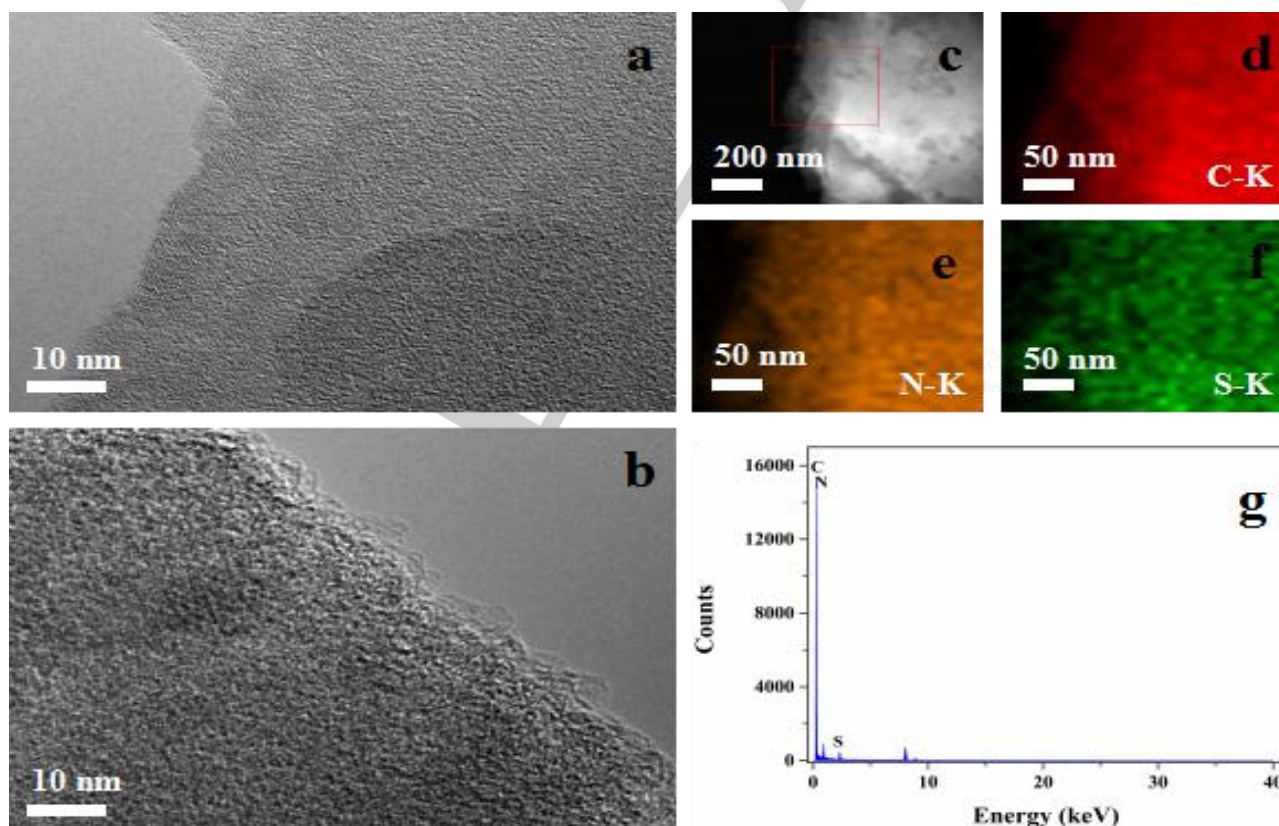
### Morphology and composition of the carbon materials

Fig. S1 showed scanning electron microscopy (SEM) images of the resulting activated carbon AC and N, S-AC-700 materials (see experimental section for preparation method). From the images of N, S-AC-700 sample, a thin and homogeneous film can be witnessed on the surface of AC (Fig. S1b). The transmission electron microscopy (TEM) results (Fig. 1) verified the presence of a uniform IL film on the surface of N, S-AC-700 (Fig. 1b) in contrast with the rough surface of AC (Fig. 1a). Additional evidences for successful impregnation of IL films were provided by element mapping images of N, S-AC-700 (Fig.

1c-g), N and S which were the typical elements of [Emim][SCN], were distributed uniformly on the carbon surface. The N and S contents were 5.69 wt% and 0.65% detected by XPS, but 4.61 wt% and 0.52 wt% by elemental analysis (EA) (Table 1), suggesting that most of the N and S atoms were on the surface of AC rather than the bulk phase.<sup>[28,38]</sup> Besides, N<sub>2</sub> adsorption-desorption experiments were conducted to measure the textural parameters of AC and N, S-AC-700, respectively. As shown in Table S1, the specific surface area of N, S-AC-700 was slightly lower than that of pure AC, which suggested that a thin film containing nitrogen and sulfur species was formed on the carbon surface after calcination under temperature of 700 °C.

**Table 1.** C, N, O, S contents determined by XPS and elemental analysis (EA) over AC and N, S-AC-700.

Sample	XPS (wt.%)				EA (wt.%)			
	C	O	N	S	C	O	N	S
AC	97.02	2.98	/	/	98.74	1.26	/	/
N, S-AC-700	91.22	2.44	5.69	0.65	93.05	1.82	4.61	0.52



**Fig. 1.** TEM images of: a) AC; b) N, S-AC-700; c-g) Elemental mapping analysis of N, S-AC-700.

## Effects of sulfur on the distribution of nitrogen species

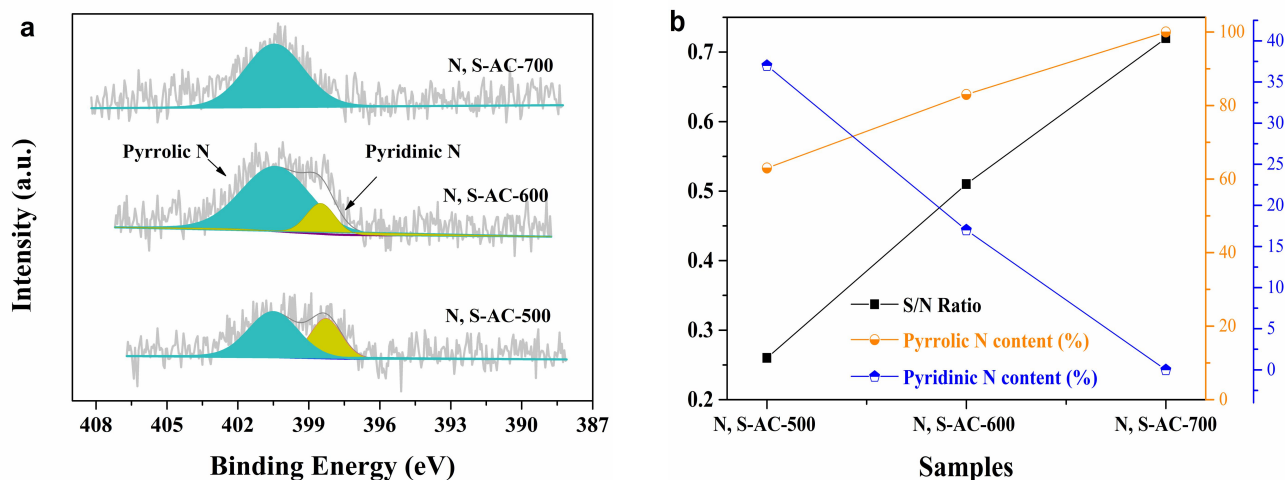


**Fig. 2.** a) N 1s XPS spectrum and b) Correlation between pyrrolic N content (%), pyridinic N content (%) and S/N ratio of: N, S-AC-500, N, S-AC-600 and N, S-AC-700.

In general, the kinds and contents of N species could be affected by the calcination temperature.<sup>[28,39,40]</sup> The coexistence of pyrrolic N and pyridinic N species in N, S-AC-500, N and N, S-AC-600 samples were evidenced by the major peaks at 400.4 eV and 398.8 eV, respectively (Fig. 2a).<sup>[38-40]</sup> The contents of pyrrolic N and pyridinic N were correlated with the S/N ratio (Fig. 2b). When the calcination temperature of N, S-AC samples was increased, the S/N ratio increased from 0.26 to 0.51 then to 0.72. The content of pyrrolic N increased from 63% to 83% and reached 100% at calcination temperature of 700 °C. Correspondingly, the pyridinic N content decreased from 37% to 17% and eventually down to 0%. As mentioned before, previous literature has proved that pyridinic N is more stable than pyrrolic N and pyrrolic N thus they can be converted to pyridinic N under temperature programmed conditions (500-700 °C).<sup>[28,31-33]</sup> But in contrast with the theoretical prediction, experimental results obtained herein showed that the content of pyridinic N in N, S-AC-700 decreased rapidly with increased temperature (Fig. 2b). Therefore, there must be a competition between sulfur species and pyridine N on the surface of activated carbon, which inhibited the formation of pyridinic N. In order to further investigate the effect of sulfur, 1-ethyl-3-methylimidazolium dicyanamide [Emim][N(CN)<sub>2</sub>], an ionic liquid that contains no sulfur but only nitrogen, was selected as a replacement for [Emim][SCN] to eliminate sulfur from the surface of the catalyst support. The catalyst synthesized using [Emim][N(CN)<sub>2</sub>] via a synthetic route identical to N, S-AC-700 was named N-AC-700. From the N 1s spectrum of N-AC-700 (Fig. S2), only evidence for the existence of pyridinic N was found, pyrrolic N was proved to be absent on the surface of N-AC-700. It is vital to explore the effect of sulfur on the formation of nitrogen species, therefore, comprehensive examination was conducted on N, S-AC-700, the catalyst sample with the lowest pyridinic N contents. On the S 2p spectrum of N, S-AC-700, peaks at 163.8 and 167.8 eV were assigned to be sulfide

groups (-C-S-C-) and oxidized sulfur groups (-C-SO<sub>x</sub>-C-), respectively (Fig. S3).<sup>[39]</sup> However, the peak corresponding to the N-S bonds (168.22 eV)<sup>[41]</sup> was not found on the spectrum of N, S-AC-700 sample (Fig. S3), which excluded the possible doping of S atoms on the pyrrolic N and pyridinic N matrix. O elements in -C-SO<sub>x</sub>-C- groups belong to the activated carbon. Content of oxygen atoms in the AC and N, S-AC-700 samples were 2.98% and 2.44% (Table 1), respectively, possible explanation for this observation is that some residual oxygen atoms might have been substituted by S atoms from -C-SO<sub>x</sub>-C- during the doping process. Therefore, we proposed that sulfur species might be able to occupy the catalytic active site where pyridinic N forms. To further reveal this mechanism at molecular level, DFT calculations were necessary.

### Catalytic performance

In order to study the catalytic performance of the prepared materials, we systematically studied a series of Au-based catalysts supported by N, S-AC materials, for acetylene hydrochlorination. Fig. 3a displayed the catalytic performance of different catalysts for hydrochlorination of acetylene under the following conditions: GHSV (C<sub>2</sub>H<sub>2</sub>) of 740 h<sup>-1</sup> at 180 °C. The selectivity of vinyl chloride (VCM) for all catalysts was over 99%. The catalytic activity of Au/N, S-AC-700 catalysts showed the highest acetylene conversion without deactivation after 10 h on stream, in contrast, the Au/AC catalyst was completely deactivated (Fig. 3a). Low acetylene conversion of pure N, S-AC-700 excluded the possible catalytic activity of sulfur and nitrogen on the carbon surface (Fig. 3a). To gain more insight into the microenvironment of the active species, we studied the kinetics of the reaction. As showed in Fig. 3b, the activation energy (*E<sub>a</sub>*) of Au/N, S-AC-700 and Au/AC were 48 and 72 kJ/mol, respectively. The large difference between activation energy of Au/N, S-AC-700 and Au/AC catalysts implied that the



active cationic gold in the catalysts may have distinct electronic environment or the reactions employing different catalysts may occur via different mechanisms.<sup>[3,42,43]</sup> Catalytic performance of Au/N, S-AC-700 catalyst was also highly dependent on the HCl/C<sub>2</sub>H<sub>2</sub> ratio (Fig. 4S). At low HCl/C<sub>2</sub>H<sub>2</sub> ratio, acetylene conversion was positively correlated to the partial pressure of hydrogen chloride (HCl/C<sub>2</sub>H<sub>2</sub> ratio), at HCl/C<sub>2</sub>H<sub>2</sub> ratio higher than 1.0/1, acetylene conversion gradually stabilized. The observation corresponds to Eley-Rideal (ER) mechanism.<sup>[27,44]</sup>

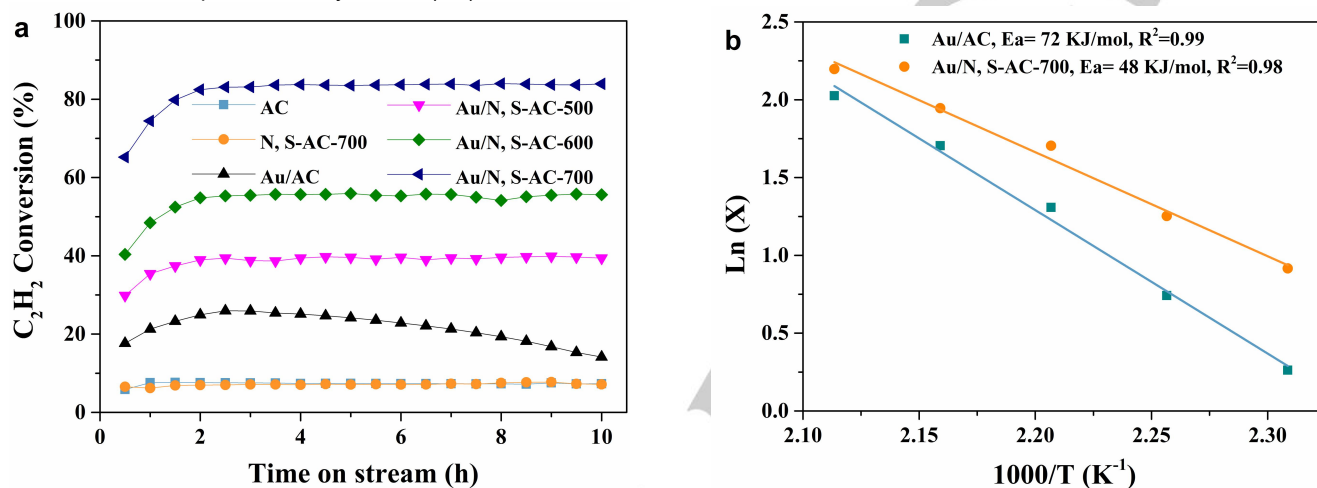


Fig. 3. a) Catalytic performance over different catalysts. Reaction conditions: Temperature= 180 °C, GHSV (C<sub>2</sub>H<sub>2</sub>)= 740 h<sup>-1</sup> and V(HCl)/V(C<sub>2</sub>H<sub>2</sub>)=1.2; b) The activation energy ( $E_a$ ) over Au/AC and Au/N, S-AC-700. X denotes for acetylene conversion in percentage.

#### Au crystal structure and chemical state analyses

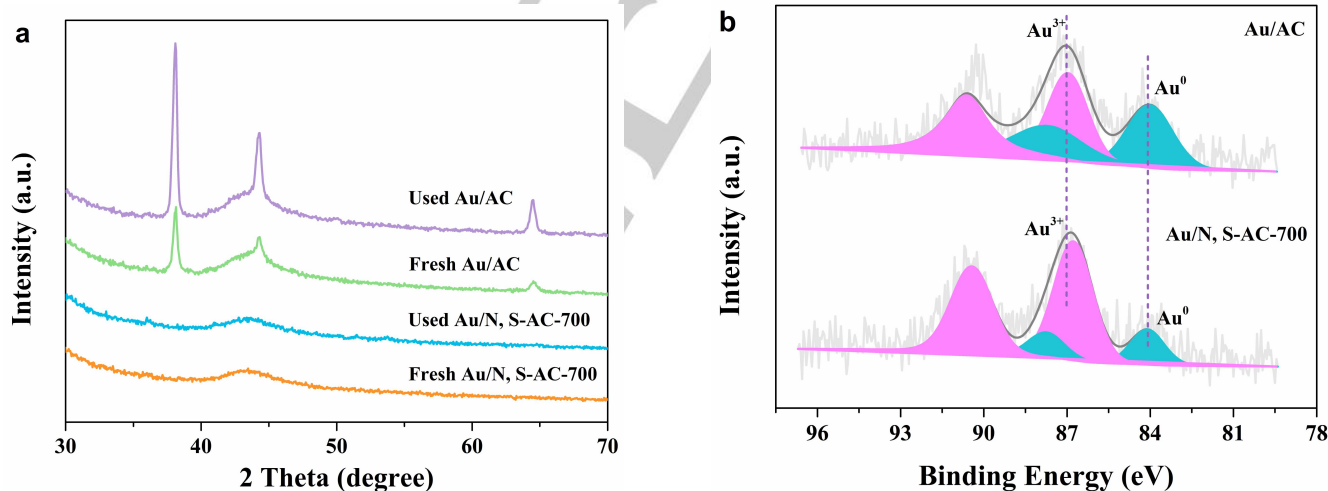


Fig. 4. a) XRD patterns of: Fresh Au/AC, Used Au/AC, Fresh Au/N, S-AC-700 and Used Au/N, S-AC-700. b) Au 4f XPS spectrum of: Fresh Au/AC and Au/N, S-AC-700.

Fig. 4a shows the XRD patterns of the fresh and used Au/AC and Au/N, S-AC-700 catalysts. According to the standard card, diffraction peaks for the (2 2 0), (2 0 0), and (1 1 1) diffraction planes of Au<sup>0</sup> should appear at 64.54°, 44.34°, and 38.12° respectively.<sup>[21]</sup> Both fresh and used Au/AC catalysts had those

The result confirmed that acetylene was first adsorbed and activated on Au/N, S-AC-700 catalyst, then reacted with gas phase HCl to form vinyl chloride (VCM). This conclusion was consistent with Hutchings' work.<sup>[2]</sup> Therefore, we believed that the lowered activation energy ( $E_a$ ) of Au/N, S-AC-700 catalyst was due to the change in the electronic environment of cationic gold.

typical characteristic peaks of Au<sup>0</sup> on their XRD patterns (Fig. 4a). Previous reports suggested that the possible reasons for Au/AC deactivation is due to the reduction of Au<sup>3+</sup> to metallic Au<sup>0</sup> via loss of Cl atoms during the reaction process.<sup>[2,21,45]</sup> This can explain the poor activity of Au/AC catalyst displayed in Fig.

3a. However, in contrast with the Au/AC catalyst, no evidence was found for the presence of metallic Au<sup>0</sup> in XRD patterns of Au/N, S-AC-700 (Fresh and Used Au/N, S-AC-700, Fig. 4a), which demonstrated that the active sites of Au<sup>3+</sup> were highly dispersed on the catalyst support, or the crystalline size of metallic Au<sup>0</sup> in the sulfur and nitrogen surface-enriched catalysts, was below the limit of XRD detection (<1.5 nm).<sup>[36]</sup> This conclusion was further verified by XPS analysis displayed in Fig. 4b. After calibration, the Au 4f<sub>7/2</sub> peaks at the binding energy of 84.0 eV and 87.0 eV were assigned to be Au<sup>0</sup> and Au<sup>3+</sup> species respectively according to the literature.<sup>[5,46]</sup> In the fresh Au/AC catalyst, the relative content of Au<sup>3+</sup> and Au<sup>0</sup> were 55% and 45%. The Au<sup>0</sup> existed in fresh Au/AC might be originated from the reduction of Au<sup>3+</sup> to Au<sup>0</sup> by the carboxyl functional groups on the carbon surface.<sup>[4,5,47]</sup> Besides, carbon with low reduction potential is also capable of reducing Au<sup>3+</sup> to Au<sup>0</sup>.<sup>[48]</sup> Compared with fresh Au/AC, the percentage of Au<sup>3+</sup> in the fresh Au/N, S-AC-700 catalyst was increased from 55% to 80%, indicating that the surface carboxylation and the reduction of Au<sup>3+</sup> by carbon was suppressed by the thin film which contains N and S formed after calcination with ionic liquid. Results for catalytic performance showed that N and S enrichment on the carbon film was beneficial for Au-based catalysts (Fig. 3a). The shift in binding energy of Au species in Au/N, S-AC-700 compared with the Au/AC catalyst provided evidence for the interactions between Au<sup>3+</sup> and N/S species. When N, S-AC-700 was used as catalyst support instead of Au/AC, the Au4f<sub>7/2</sub> signals corresponding to Au<sup>3+</sup> was negative shifted from 87.0 eV (Au/AC, Fig.4b) to 86.5 eV (Au/N, S-AC-700, Fig.4b), while the metallic Au<sup>0</sup> signals of the catalysts were only slightly changed (Au/N, S-AC-700, 84.0 eV vs. Au/AC, 84.1 eV, Fig. 4b). Meanwhile, the same changes were noted for N, S-AC-700, the peak corresponding to pyrrolic N of Au/N, S-AC-700 catalyst was 0.4 eV higher than the standard BE of 400.4 eV (Fig. S5).<sup>[38-40]</sup> Reduction on the reaction activation energy (Fig. 3b) and the negative shift of Au<sup>3+</sup> binding energy (Fig. 4b) caused by doping of heteroatoms can be ascribed to the electrons transferred from pyrrolic N to the Au<sup>3+</sup> center, thus the formation of a complex between Au<sup>3+</sup> and pyrrolic N via π-σ coordination bond. This proposal was supported by results acquired from activity evaluation experiments, catalytic activities of the catalysts was proportional to the pyrrolic N content (Fig. 5). Similar observations have also been reported in previous study.<sup>[21]</sup> It should be noted that the catalytic performance of Au/N-AC-700 (not shown) was comparable to that of Au/AC, suggesting that pyridinic N may have no effect on the catalytic performance.

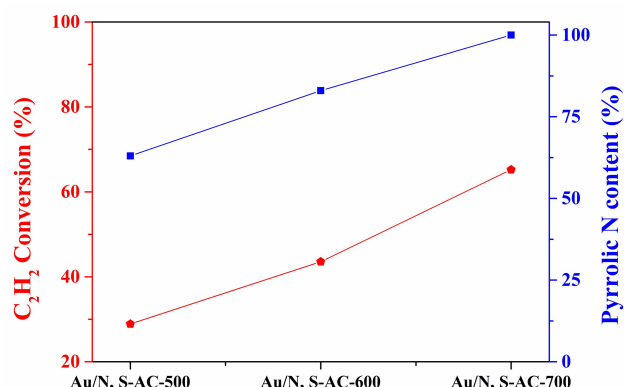
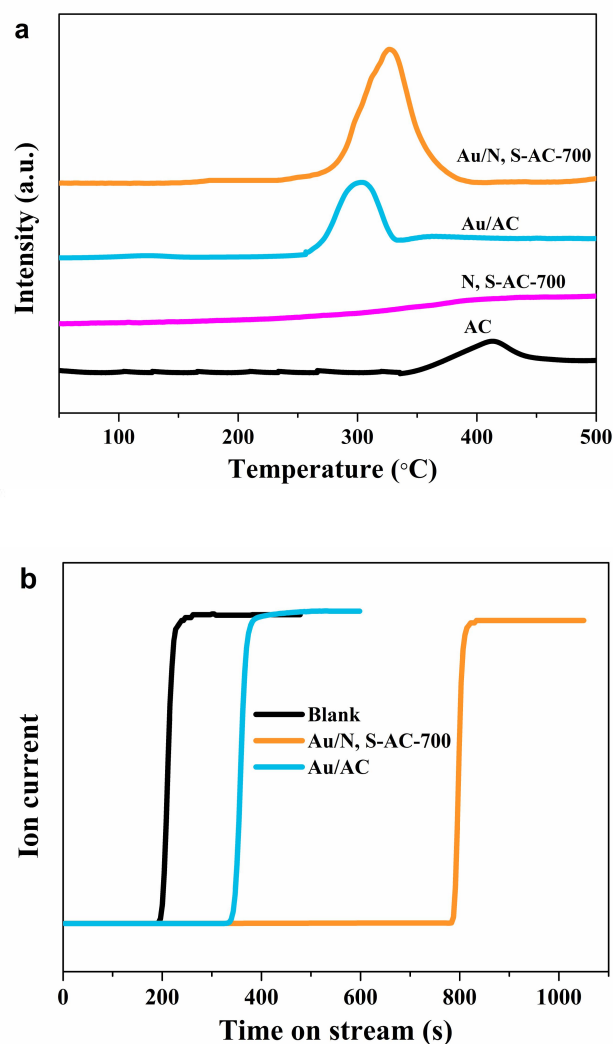


Fig. 5. Correlation between acetylene conversion (%) and pyrrolic N content (%) for Au/N, S-AC-500, Au/N, S-AC-600 and Au/N, S-AC-700.

#### Reducibility and Adsorption property of the reactants



**Fig. 6.** a) H<sub>2</sub>-TPR profiles of: Au/N, S-AC-700, Au/AC, N, S-AC-700 and AC; b) HCl-Breakthrough profiles of: N, S-AC-700 (Blank), Au/AC and Au/N, S-AC-700.

The reducibility and adsorption property of the substrates on catalysts could be affected via the changing microenvironment of active sites. H<sub>2</sub>-temperature programmed reduction (H<sub>2</sub>-TPR) was a powerful technique for characterizing and analyzing heterogeneous catalysts.<sup>[49,50]</sup> The reduction peaks at 300 °C for Au/AC and 352 °C for Au/N, S-AC-700 were attributed to the reduction of cationic Au<sup>3+</sup> species (Fig. 6a).<sup>[5,6]</sup> The higher reduction temperature of Au/N, S-AC-700 compared to that of Au/AC confirmed that strong interaction between pyrrolic N and Au can significantly inhibit the reduction of Au<sup>3+</sup>. In addition, the broad H<sub>2</sub> consumption peak for fresh Au/N, S-AC-700 was stronger than that for fresh Au/AC catalyst which illustrated that cationic Au species fixed on the surface of Au/N, S-AC-700 were more abundant than that on the surface of Au/AC catalyst, consistent with the results obtained from XPS analysis mentioned before (Fig. 4b). For the catalyst support AC, appearance of the reduction peak at 410 °C (Fig. 6a) could be explained by the reaction between active Au<sup>3+</sup> and carboxylic groups on the surface of AC (C-COOH + Au<sup>3+</sup> → C + Au<sup>0</sup> + H<sup>+</sup> + CO<sub>2</sub>).<sup>[21]</sup> In contrast with AC, N, S-AC-700 showed no reduction peak near that area (Fig. 6a). A possible rationalization for the observations described above is that the pyrrolic N-enriched carbon film coated on the surface of the carbon support can serve as a protective layer for the cationic gold species, besides, presence of -C-SO<sub>x</sub>-C- groups can prevent the reaction between Au<sup>3+</sup> and carboxylic groups from happening. Adsorption properties of hydrogen chloride on different Au-based catalysts were studied based on the Breakthrough curve (Fig. 6b). Adsorption capacity of substrates over active sites of catalysts can be reflected on the Breakthrough time,<sup>[51]</sup> therefore, Fig. 6b proved that Au/N, S-AC-700 was capable of adsorbing more HCl than Au/AC. As proved by XPS analysis, coordination with electron-donating pyrrolic N groups can increase the electron density on the Au (III) center and thereby causes the superior adsorption capacity of Au/N, S-AC-700 catalyst. In addition, during acetylene hydrochlorination, AuCl<sub>4</sub><sup>-</sup> can react with C<sub>2</sub>H<sub>2</sub> hence triggers a constant loss of Cl atoms from AuCl<sub>4</sub><sup>-</sup> leading to catalyst deactivation. However, AuCl<sub>3</sub> is a good electron acceptor which is willing to take one Cl<sup>-</sup> ion from HCl,<sup>[52]</sup> therefore, sufficient supply of HCl can effectively improve the catalytic performance of Au/N, S-AC-700 catalyst (Fig. 1). Furthermore, the adsorption HCl on the active Au<sup>3+</sup> could further activate the adsorbed C<sub>2</sub>H<sub>2</sub>, leading to a decrease in the activation energy of the reaction (Fig. 2b).<sup>[3]</sup>

### Au sintering by HCl

General role of HCl in the hydrochlorination reaction of acetylene is to activate and oxidize gold catalysts.<sup>[53]</sup> However, HCl is also the culprit for the sintering problem of Au particles which is another major cause of catalyst deactivation in acetylene hydrochlorination. Au crystalline has been reported to sinter rapidly at 21 nm after only five minutes of exposure to

HCl,<sup>[36]</sup> consistent with the results obtained for Au/AC catalyst (Fig. S6). However, Au/N, S-AC-700 catalyst showed excellent resistance to the sintering effect, no evidence was found for the presence of Au<sup>0</sup> nanoparticles even after 60 min of exposure to HCl (Fig. S6). Furthermore, for Au/N, S-AC-700 catalyst, sintering of Au was inhibited throughout the reaction since no obvious difference was witnessed between XRD patterns of used and fresh Au/N, S-AC-700 catalysts (Fig. 4a). Cause of sintering effect is the mobility of the Au species on the carbon surface. But in Au/N, S-AC-700 catalyst, Au species may have been fixed in position by the strong interaction between Au<sup>3+</sup> cation and pyrrolic N, hence sintering effect is inhibited for it.

### Long-term stability of Au/N, S-AC-700 catalyst

Despite its excellent performance, cost of gold-based catalysts has greatly limited its industrial application in comparison with the commercially favourable Hg/AC catalyst for PVC production.<sup>[45]</sup> Possibility of using Au/N, S-AC-700 catalyst instead of Hg/AC catalyst in industrial PVC production was evaluated by using Au/N, S-AC-700 catalyst with catalyst loading of 0.1 wt.% (10 times lower) under industrial reaction conditions for 300 h (Fig. 7). The highest acetylene conversion was 99.2%, and the selectivity to VCM was approximately 99.6%. The acetylene conversion decreased slightly to 98.2% after 300 h on stream. Owing to the nitrogen and sulfur in the carbon catalyst support, Au/N, S-AC-700 catalyst exhibited superior stability for acetylene hydrochlorination.

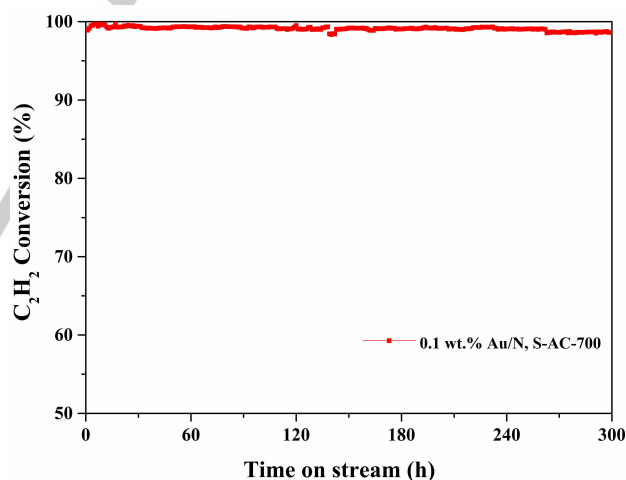


**Fig. 7.** A long-term catalytic performance evaluation of 0.1 wt.% Au/N, S-AC-700 catalyst. Reaction conditions: Temperature= 180 °C, GHSV (C<sub>2</sub>H<sub>2</sub>)= 30 h<sup>-1</sup> and V(HCl)/V(C<sub>2</sub>H<sub>2</sub>)=1.2.

### Conclusions

In conclusion, Au catalyst supported on the activated carbon with nitrogen and sulfur-doped surface, was successfully prepared and assessed for acetylene hydrochlorination. During the investigation, we noticed that coordination between the π electrons on pyrrolic N and the Au(III) center can efficiently increase the electron density of gold hence facilitate the

adsorption of HCl and suppress the reduction of active Au species by C<sub>2</sub>H<sub>2</sub>, resulting in superior activity and stability of Au/N, S-AC-700 catalyst. Presence of sulfur species on the carbon surface was considered to be able to inhibit the formation of undesirable pyridinic N species. Most importantly, our Au/N, S-AC-700 catalyst has been proved to be a strong competitor to the commercial Hg/AC catalyst in industrial acetylene hydrochlorination.

## Experimental Section

### Catalyst Preparation

The activated carbon (NORIT ROX 0.8) was first pretreated with 1-ethyl-3-methylimidazolium thiocyanate ([Emim][SCN]), (Lanzhou Green chem Co., Ltd., 99%) for 12 h. The obtained mixture was then thermally treated in N<sub>2</sub> atmosphere at 500, 600 and 700 °C to obtain N, S-AC-500, N, S-AC-600 and N, S-AC-700, respectively. As a representative, the obtained N, S-AC-700 sample and H<sub>2</sub>SO<sub>4</sub> was dissolved in deionized water. Subsequently, the impregnated sample was laid overnight. Finally, the sample was dried at 110 °C for 16 h under nitrogen flow to obtain the catalyst, labeled as Au/N, S-AC-700 with a nominal Au loading of 1 wt.%.

### Catalytic reaction evaluation

The catalytic performance was monitored in a fixed-bed micro-reactor (10 mm diameter). After the catalyst was loaded into the reactor, the reactor was heated up to the reaction temperature at a ramp rate of 10 °C/min and held for 30 min under nitrogen atmosphere. Then, the C<sub>2</sub>H<sub>2</sub>/HCl mixed gas was fed into the reactor under ambient pressure. The effluent gas mixture from the reactor was flew through a bubbler containing aqueous sodium hydroxide solution to remove any unreacted hydrogen chloride and the resulting gas was then analyzed by gas chromatography to calculate the acetylene conversion and VCM selectivity.

### Characterization of catalysts

Scanning electron microscopy (SEM) morphology was evaluated with a Philips XL-30 scanning electron microscope. Transmission electron microscopy (TEM) analysis was performed on a Tecnai G2 F30 S-Twin, operating at an acceleration voltage of 300 kV. Nitrogen adsorption/desorption isotherms was performed using a Micromeritics ASAP 2020 instrument. X-ray diffraction (XRD) measurements were obtained using a PANalytical-X'Pert PRO generator with Cu K $\alpha$  radiation ( $\lambda = 0.1541$  nm). X-ray photoelectron spectroscopy (XPS) was performed on a Kratos AXIS Ultra DLD spectrometer with monochromatized aluminum X-ray source (1486.6 eV). Temperature-programmed reduction (TPR) was carried out in a micro-flow reactor fed with hydrogen (10% in Ar) at a flow rate of 45 mL min<sup>-1</sup>. The HCl-Breakthrough profiles were performed on an Omnistar GSD320 (Pfeiffer Vacuum, Germany) mass spectrometer.

## Acknowledgements

We gratefully acknowledge that the financial support was provided by the National Natural Science Foundation of China (NSFC; Grant 21606199, 21476207).

**Keywords:** Nitrogen-doped carbons • pyrrolic nitrogen • pyridinic nitrogen • Au/N, S-AC-700 • acetylene hydrochlorination

- [1] P. Johnston, N. Carthey, G. J. Hutchings, *J. Am. Chem. Soc.* **2015**, *137*, 14548-14557.
- [2] G. Malta, S. A. Kondrat, S. J. Freakley, C. J. Davies, L. Lu, S. Dawson, A. Theftord, E. K. Gibson, D. J. Morgan, W. Jones, P. P. Wells, P. Johnston, C. R. A. Catlow, C. J. Kiely, G. J. Hutchings, *Science* **2017**, *355*, 1399-1403.
- [3] B. Wang, H. Lai, Y. Yue, G. Sheng, Y. Deng, H. He, L. Guo, J. Zhao, X. Li, *Catal.* **2018**, *8*, 351.
- [4] G. Malta, S. A. Kondrat, S. J. Freakley, C. J. Davies, S. Dawson, X. Liu, L. Lu, K. Dymkowski, F. Fernandez-Alonso, S. Mukhopadhyay, E. K. Gibson, P. P. Wells, S. F. Parker, C. J. Kiely, G. J. Hutchings, *ACS Catal.* **2018**, *8*, 8493-8505.
- [5] J. Zhao, B. Wang, Y. Yue, S. Di, Y. Zhai, H. He, G. Sheng, H. Lai, Y. Zhu, L. Guo, X. Li, *J. Catal.* **2018**, *365*, 153-162.
- [6] J. Zhao, B. Wang, X. Xu, Y. Yu, S. Di, H. Xu, Y. Zhai, H. He, L. Guo, Z. Pan, X. Li, *J. Catal.* **2017**, *350*, 149-158.
- [6] M. Conte, A. Carley, G. Attard, A. Herzing, C. Kiely, G. Hutchings, *J. Catal.* **2008**, *257*, 190-198.
- [7] Q. L. Song, S. J. Wang, B. X. Shen, J. G. Zhao, *Pet. Sci. Technol.* **2010**, *28*, 1825-1833.
- [9] Y. Pu, J. Zhang, L. Yu, Y. Jin, W. Li, *App. Catal., A* **2014**, *488*, 28-36.
- [10] H. Zhang, W. Li, Y. Jin, W. Sheng, M. Hu, X. Wang, J. Zhang, *Appl. Catal., B* **2016**, *189*, 56-64.
- [11] J. Zhang, W. Sheng, C. Guo, W. Li, *RSC Adv.* **2013**, *3*, 21062.
- [12] Y. Jin, G. Li, J. Zhang, Y. Pu, W. Li, *RSC Adv.* **2015**, *5*, 37774-37779.
- [13] B. Kumar, G. K. Rao, S. Saha, A. K. Ganguli, *Chem. Phys. Chem.* **2016**, *17*, 155-161.
- [14] J. Xu, J. Zhao, T. Zhang, X. Di, S. Gu, J. Ni, X. Li, *RSC Adv.* **2015**, *5*, 38159-38163.
- [15] Y. Zhai, J. Zhao, X. Di, S. Di, B. Wang, Y. Yue, G. Sheng, H. Lai, L. Guo, H. Wang, X. Li, *Catal. Sci. Technol.* **2018**, *8*, 2901-2908.
- [16] H. Xu, G. Luo, *J. Ind. Eng. Chem.* **2018**, *65*, 13-25.
- [17] M. Conte, C. J. Davies, D. J. Morgan, T. E. Davies, D. J. Elias, A. F. Carley, P. Johnston, G. J. Hutchings, *J. Catal.* **2013**, *297*, 128-136.
- [18] J. Zhao, S. Gu, X. Xu, T. Zhang, Y. Yu, X. Di, J. Ni, Z. Pan, X. Li, *Catal. Sci. Technol.* **2016**, *6*, 3263-3270.
- [19] H. Zhang, B. Dai, X. Wang, W. Li, Y. Han, J. Gu, J. Zhang, *Green Chem.* **2013**, *15*, 829.
- [20] K. Zhou, W. Wang, Z. Zhao, G. Luo, J. T. Miller, M. S. Wong, F. Wei, *ACS Catal.* **2014**, *4*, 3112-3116.
- [21] X. Li, M. Zhu, B. Dai, *Appl. Catal., B* **2013**, *142-143*, 234-240.
- [22] W. Gong, F. Zhao, L. Kang, *Comput. Theor. Chem.* **2018**, *1130*, 83-89.
- [23] P. Li, M. Ding, L. He, K. Tie, H. Ma, X. Pan, X. Bao, *Sci. Chin. Chem.* **2018**, *61*, 444-448.
- [24] J. Zhao, J. Xu, J. Xu, T. Zhang, X. Di, J. Ni, X. Li, *Chem. Eng. J.* **2015**, *262*, 1152-1160.
- [25] J. Zhao, T. Zhang, X. Di, J. Xu, J. Xu, F. Feng, J. Ni, X. Li, *RSC Adv.* **2015**, *5*, 6925-6931.
- [26] X.-X. Di, J. Zhao, Y. Yu, X.-L. Xu, S.-C. Gu, H.-H. He, T.-T. Zhang, X.-N. Li, *Chin. Chem. Lett.* **2016**, *27*, 1567-1571.
- [27] X. Li, X. Pan, L. Yu, P. Ren, X. Wu, L. Sun, F. Jiao, X. Bao, *Nat. Commun.* **2014**, *5*, 3688.
- [28] M. Inagaki, M. Toyoda, Y. Soneda, T. Morishita, *Carbon* **2018**, *132*, 104-140.
- [29] W. Zhang, Z. Chen, X. Guo, K. Jin, Y. Wang, L. Li, Y. Zhang, Z. Wang, L. Sun, T. Zhang, *Electrochim. Acta* **2018**, *278*, 51-60.



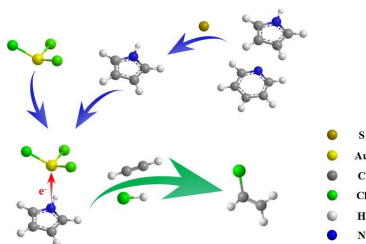
- [30] L. Lai, J. R. Potts, D. Zhan, L. Wang, C. K. Poh, C. Tang, H. Gong, Z. Shen, J. Lin, R. S. Ruoff, *Energy Environ. Sci.* **2012**, *5*, 7936.
- [31] Y. Tian, J. Zhang, W. Zuo, L. Chen, Y. Cui, T. Tan, *Environ. Sci. Technol.* **2013**, *47*, 3498-3505.
- [32] L. Wei, L. Wen, T. Yang, N. Zhang, *Energy & Fuels* **2015**, *29*, 5088-5094.
- [33] X. Jiang, H. Shi, J. Shen, W. Han, X. Sun, J. Li, L. Wang, *J. Electroanal. Chem.* **2018**, *823*, 32-39.
- [34] X. Zhao, S. Li, H. Cheng, J. Schmidt, A. Thomas, *ACS Appl. Mat. Inter.* **2018**, *10*, 3912-3920.
- [35] M. Conte, C. J. Davies, D. J. Morgan, T. E. Davies, A. F. Carley, P. Johnston, G. J. Hutchings, *Catal. Sci. Technol.* **2013**, *3*, 128-134.
- [36] K. C. O'Connell, J. R. Monnier, J. R. Regalbuto, *Appl. Catal., B* **2018**, *225*, 264-272.
- [37] S. Di, Y. Xu, Q. Zhang, X. Xu, Y. Zhai, B. Wang, H. He, Q. Wang, H. Xu, Y. Jiang, J. Zhao, X. Li, *RSC Adv.* **2018**, *8*, 24094-24100.
- [38] O. S. G. P. Soares, R. P. Rocha, A. G. Gonçalves, J. L. Figueiredo, J. J. M. Órfão, M. F. R. Pereira, *Carbon* **2015**, *91*, 114-121.
- [39] X. Dong, S. Chao, F. Wan, Q. Guan, G. Wang, W. Li, *J. Catal.* **2018**, *359*, 161-170.
- [40] R. Lin, S. K. Kaiser, R. Hauert, J. Pérez-Ramírez, *ACS Catal.* **2018**, *8*, 1114-1121.
- [41] G.-l. Zhuang, J.-q. Bai, X.-y. Tao, J.-m. Luo, X.-d. Wang, Y.-f. Gao, X. Zhong, X.-n. Li, J.-g. Wang, *J. Mat. Chem. A* **2015**, *3*, 20244-20253.
- [42] H. Xu, J. Si, G. Luo, *Inter. J. Chem. React. Eng.* **2017**, *15*.
- [43] W. D. Michalak, J. M. Krier, S. Alayoglu, J.-Y. Shin, K. An, K. Komvopoulos, Z. Liu, G. A. Somorjai, *J. Catal.* **2014**, *312*, 17-25.
- [44] P. Li, H. Li, X. Pan, K. Tie, T. Cui, M. Ding, X. Bao, *ACS Catal.* **2017**, *7*, 8572-8577.
- [45] J. Zhong, Y. Xu, Z. Liu, *Green Chem.* **2018**, *20*, 2412-2427.
- [46] D. Hu, L. Wang, F. Wang, J. Wang, *Catal. Commun.* **2018**, *115*, 45-48.
- [47] J. Zhao, J. Ni, J. Xu, J. Xu, J. Cen, X. Li, *Catal. Commun.* **2014**, *54*, 72-76.
- [48] J. Xi, H. Sun, D. Wang, Z. Zhang, X. Duan, J. Xiao, F. Xiao, L. Liu, S. Wang, *Appl. Catal., B* **2018**, *225*, 291-297.
- [49] J. Zhao, J. Xu, J. Xu, J. Ni, T. Zhang, X. Xu, X. Li, *ChemPlusChem* **2015**, *80*, 196-201.
- [50] H. Li, B. Wu, F. Wang, X. Zhang, *ChemCatChem* **2018**, *10*, 4090-4099.
- [51] Z. Song, G. Liu, D. He, X. Pang, Y. Tong, Y. Wu, D. Yuan, Z. Liu, Y. Xu, *Green Chem.* **2016**, *18*, 5994-5998.
- [52] H. Xu, K. Zhou, J. Si, C. Li, G. Luo, *Catal. Sci. Technol.* **2016**, *6*, 1357-1366.
- [53] M. Conte, A. F. Carley, G. J. Hutchings, *Catal. Lett.* **2008**, *124*, 165-167.

Entry for the Table of Contents (Please choose one layout)

Layout 1:

## FULL PAPER

A carbon surface with pyrrolic N enriched materia was developed in terms of "atom economy" and "green chemistry". The presence of sulfur species on the carbon surface inhibited the formation of pyridinic N which was not necessary for the hydrochlorination of acetylene.



*Bolin Wang, Jia Zhao\*, Yuxue Yue, Gangfeng Sheng, Huixia Lai, Jiayao Rui, Haihua He, Zhongting Hu, Feng Feng, Qunfeng Zhang, Lingling Guo, Xiaonian Li\**

**Page No. – Page No.**

**Title**

**Carbon with Surface-Enriched Nitrogen and Sulfur Supported Au Catalysts for Acetylene Hydrochlorination**